DALTON
FULL PAPER

Spin frustration in the butterfly-like tetrameric $[Ni_4(\mu\text{-}CO_3)_2(aetpy)_8][ClO_4]_4$ [aetpy = (2-aminoethyl)pyridine] complex. Structure and magnetic properties

Albert Escuer,*[a] Ramon Vicente,[a] Sujit B. Kumar[a] and Franz A. Mautner[b]

[a] *Departament de Química Inorgànica, Universitat de Barcelona, Diagonal 647, 08028 Barcelona, Spain. E-mail: http://www.ub.es/inorgani/molmag.htm*
[b] *Institut für Physikalische und Theoretische Chemie, Technische Universität Graz, A-8010 Graz, Austria*

Received 19th May 1998, Accepted 10th August 1998

A new tetranuclear nickel compound, showing $\mu\text{-}CO_3$ bridges and butterfly topology has been synthesised and structurally characterised. The complex $[Ni_4(\mu\text{-}CO_3)_2(aetpy)_8][ClO_4]_4$, where aetpy corresponds to (2-aminoethyl)-pyridine, crystallises in the tetragonal system, space group $P4(2)2(1)2$ (no. 94), $a = 14.523(4)$, $c = 16.566(5)$ Å and $Z = 8$. Magnetic measurements show an overall antiferromagnetic behaviour with a quasi-degenerate set of spin levels $S = 0$, $S = 1$ and $S = 2$ as a ground state, which may be rationalised in terms of a spin frustration system.

The fixation of atmospheric CO_2 by basic solutions of first-row transition complexes, through hydroxo intermediates, has received considerable attention in the past few years in relation to bioinorganic models or catalytic applications. The co-ordination chemistry of the carbonate anion is characterised by its extreme versatility, and twelve kinds of $\mu\text{-}CO_3$ bridge have been described to date. From the magnetic point of view, a wide range of properties have been characterised [mainly for copper(II) polynuclear systems[1]], allowing ferro- or antiferromagnetic coupling depending on the co-ordination mode.

For the nickel ion, few carbonate-bridged polynuclear systems have been reported, although fixation of atmospheric CO_2 by nickel derivatives has been studied systematically for N-alkyl-substituted ethane-1,2-diamine[2] or propane-1,3-diamine.[3] Effective CO_2 fixation was obtained only by using *N*,*N*-dimethylethane-1,2-diamine or 2,2-dimethylpropane-1,3-diamine and perchlorate as counter anion. In addition to these systematic studies, several isolated compounds have been characterised.[4]

Only three co-ordination modes have been described for the carbonate ion when it acts as a bridge in polynuclear nickel compounds. The bis-bidentate mode **a** (the most common)[4a–e] and **b** (one compound)[4f] are characterised by strong antiferromagnetic coupling, due to the large Ni–O–Ni bond angle (typical J values close to -80 cm^{-1}), whereas for the only example of **c** co-ordination, weak antiferromagnetic coupling ($J = -7.8$ cm^{-1}) was found.[3]

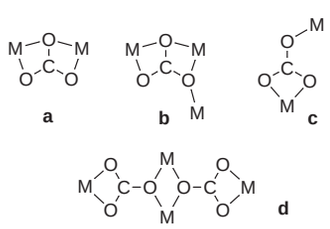

Following our study on the polynuclear nickel–carbonate system, a new butterfly tetranuclear $[Ni_4(\mu\text{-}CO_3)_2(aetpy)_8][ClO_4]_4$ derivative was obtained by reaction of basic solutions of (2-aminoethyl)pyridine (aepty) and nickel(II) cation with atmospheric CO_2. The $[Ni_4(\mu\text{-}CO_3)_2(aetpy)_8]^{4+}$ unit shows the same metal–carbonate skeleton, **d**, as $[Ti_4(Cp)_8(\mu\text{-}CO_3)_2]$,[5] and may be assumed to act as a double **c** bridged complex.

The $[Ni_4(\mu\text{-}CO_3)_2(aetpy)_8][ClO_4]_4$ compound shows two interesting features as a result of the nuclearity: a) whereas the butterfly arrangement has often been found for manganese or iron compounds it is rare for nickel(II). Tetranuclear compounds of nickel commonly show the Ni_4O_4 cubane core[6] or in some rare cases the Ni_4N_4 cubane arrangement.[7] More or less distorted square topology has also been found for different bridging ligands,[8] but linear or butterfly topologies are uncommon. To our knowledge, only two nickel butterfly fragments have been characterised to date, the $[Ni_4(H_2O)_2(P_2W_{15}O_{56})_2]^{16-}$ polyanion[9] and $[Ni_4(L)_2(pz)_2(CH_3OH)]$ [L = 2,6-bis(salicylideneaminomethyl)-4-methylphenol, pz = pyrazolyl],[10] for which two of the nickel atoms show a square-planar environment. b) The reported tetranuclear nickel compounds for which susceptibility experiments have been performed show, in all cases, ferromagnetic interactions with ground state $S_T = 4$, or antiferromagnetic interactions allowing an $S_T = 0$ ground state. The magnetic measurements for $[Ni_4(\mu\text{-}CO_3)_2(aetpy)_8][ClO_4]_4$ indicate antiferromagnetic interactions for the two superexchange pathways present in the molecule, the "body" oxo bridge and the "body-wing" **c**-type bridges. The experimental ratio between the two superexchange coupling constants lies in the spin frustration range, in which one $S = 0$, one $S = 1$ and one $S = 2$ ground states are formally degenerate as discussed below.

Here, we present the structural and magnetic properties of $[Ni_4(\mu\text{-}CO_3)_2(aetpy)_8][ClO_4]_4$, together with the expected behaviour of the nickel(II) butterfly ground state as a function of the coupling constants.

Experimental

Synthesis

CAUTION: Perchlorate salts of metal complexes with organic ligands are potentially explosive. Only a small amount of material should be prepared, and it should be handled with caution. $[Ni_4(\mu\text{-}CO_3)_2(aetpy)_8][ClO_4]_4$ may be synthesised by either of two similar procedures: an aqueous solution of nickel perchlorate hexahydrate (1 mmol) and (2-aminoethyl)pyridine (3 mmol) or an aqueous solution of nickel perchlorate hexahydrate (1 mmol), (2-aminoethyl)pyridine (2 mmol) and diethylamine (2 mmol) were stirred vigorously during 24 h to permit the basic solutions to react with atmospheric CO_2. The solutions were then left to evaporate and a blue crystalline

compound was obtained. Recrystallization from water–ethanol yields well formed blue crystals of $[Ni_4(aetpy)_8(\mu\text{-}CO_3)_2][ClO_4]_4$ [$C_{58}H_{80}Cl_4N_{16}Ni_4O_{22}$: Calc.(Found): C, 40.26(40.2); H, 4.67(4.6); N, 12.96(13.0); Cl, 8.20(8.4)%]. In addition to the typical bands of the aetpy ligand and the perchlorate counter anion in the IR spectrum, a strong absorption was also observed at 1415 cm^{-1} due to the co-ordinated carbonate ion.

Spectral and magnetic measurements

Infrared spectra (4000–400 cm^{-1}) were recorded from KBr pellets on a Nicolet 520 FTIR spectrophotometer. Magnetic measurements were carried out with a DSM8 pendulum susceptometer, working in the temperature range 4–300 K. Low temperature susceptibility data and high field magnetisation measurements were performed with a SQUID device. Diamagnetic corrections were estimated from Pascal tables.

X-Ray crystallography

Crystal data. $C_{14.5}H_{20}ClN_4NiO_{5.5}$, $M = 432.51$, tetragonal, $a = 14.523(4)$, $c = 16.566(5)$ Å, $U = 3494(2)$ Å^3, $T = 295(2)$ K, space group $P4(2)2(1)2$ (no. 94), $Z = 8$, μ(Mo-Kα) = 1.301 mm^{-1}, reflections measured 3539, 2765 unique ($R_{int} = 0.0470$) which were used in all calculations. The final $wR(F^2)$ was 0.1293, $R1 = 0.0531$.

The single crystal data were collected on a modified STOE four-circle diffractometer. Crystal size: 0.60 × 0.50 × 0.30 mm. Graphite-monochromatised Mo-Kα radiation ($\lambda = 0.710\ 69$ Å), using the ω-scan technique to collect the data. The accurate unit-cell parameters were determined from automatic centring of 67 reflections ($10.8 < \theta < 13.7°$) and refined by least-squares methods. Range for data collection $2.80 < \theta < 25.98°$. No significant intensity decay in three control reflections (−1 −1 −2; 2 −2 1; 1 6 1), measured every hour, was observed. Corrections were applied for Lorentz-polarisation effects and for absorption[11] (range of normalised transmission coefficients: 0.360–1.000). The structure was solved by direct methods using the SHELXS 86 computer program,[12] and refined by full-matrix least-squares methods on F^2, using the SHELXL 93 computer program[13] incorporated in SHELXTL/PC V 5.03 program package.[14] All non-hydrogen atoms were refined anisotropically. The hydrogen atoms of the pyridine rings and CH_2 groups were located on calculated positions and their isotropic displacement parameters were fixed with the equivalent U values of the parent C atoms. Hydrogen atoms of the NH_2 groups were obtained from Fourier-difference maps and included in final refinement cycles by use of distance restraints and applying two common isotropic displacement factors. Rigid group restraints were also applied for the disordered perchlorate counter anion with Cl(2) located in special position 4e. Number of refined parameters 271. Absolute structure parameter −0.02(3).[15] Goodness-of-fit: 1.070. Maximum and minimum peaks in the final Fourier-difference synthesis were 0.508 and −0.564 e Å^{-3}. Significant bond parameters are given in Table 1.

CCDC reference number 186/1122.

Results and discussion

Crystal structure

The atom labelling scheme is shown in Fig. 1. The structure consists of tetrameric $[Ni_4(CO_3)_2(aetpy)_8]^{4+}$ units and the corresponding perchlorate counter anions. Each nickel atom shows octahedral *cis* co-ordination to two (ethylamino)pyridine bidentate ligands and two oxygen atoms from the carbonate bridges. The nickel–carbonate skeleton shows a butterfly arrangement in which the body is formed by the planar Ni(1)–

Table 1 Selected bond lengths (Å) and angles (°) for $[Ni_4(\mu\text{-}CO_3)_2(aetpy)_8][ClO_4]_4$

Ni(1)–N(1)	2.168(4)	Ni(2)–N(3)	2.147(5)
Ni(1)–N(2)	2.085(4)	Ni(2)–N(4A)	2.061(6)
Ni(1)–O(1)	2.181(3)	Ni(2)–O(2)	2.123(4)
C(1)–O(1)	1.286(8)	C(1)–O(2)	1.281(5)
Ni(1) · · · Ni(1A)	3.468(1)	Ni(1) · · · Ni(2)	5.386(2)
N(1)–Ni(1)–N(1B)	174.8(2)	N(3)–Ni(2)–N(3C)	179.5(3)
N(1)–Ni(1)–N(2)	90.2(2)	N(3)–Ni(2)–N(4)	89.4(3)
N(1)–Ni(1)–N(2B)	86.2(2)	N(3)–Ni(2)–N(4C)	90.3(2)
N(1)–Ni(1)–O(1)	93.93(14)	N(3)–Ni(2)–O(2)	87.7(2)
N(1)–Ni(1)–O(1A)	90.23(14)	N(3)–Ni(2)–O(2C)	92.7(2)
N(2)–Ni(1)–N(2B)	91.8(3)	N(4)–Ni(2)–N(4C)	104.3(4)
N(2)–Ni(1)–O(1)	170.6(2)	N(4)–Ni(2)–O(2)	158.5(2)
N(2)–Ni(1)–O(1A)	96.9(2)	N(4)–Ni(2)–O(2C)	97.0(2)
O(1)–Ni(1)–O(1B)	74.7(2)	O(2)–Ni(2)–O(2C)	61.9(2)
Ni(1)–O(1)–Ni(1A)	105.3(2)		
O(1)–C(1)–O(2)	121.5(3)		
O(2)–C(1)–O(2C)	117.0(6)		

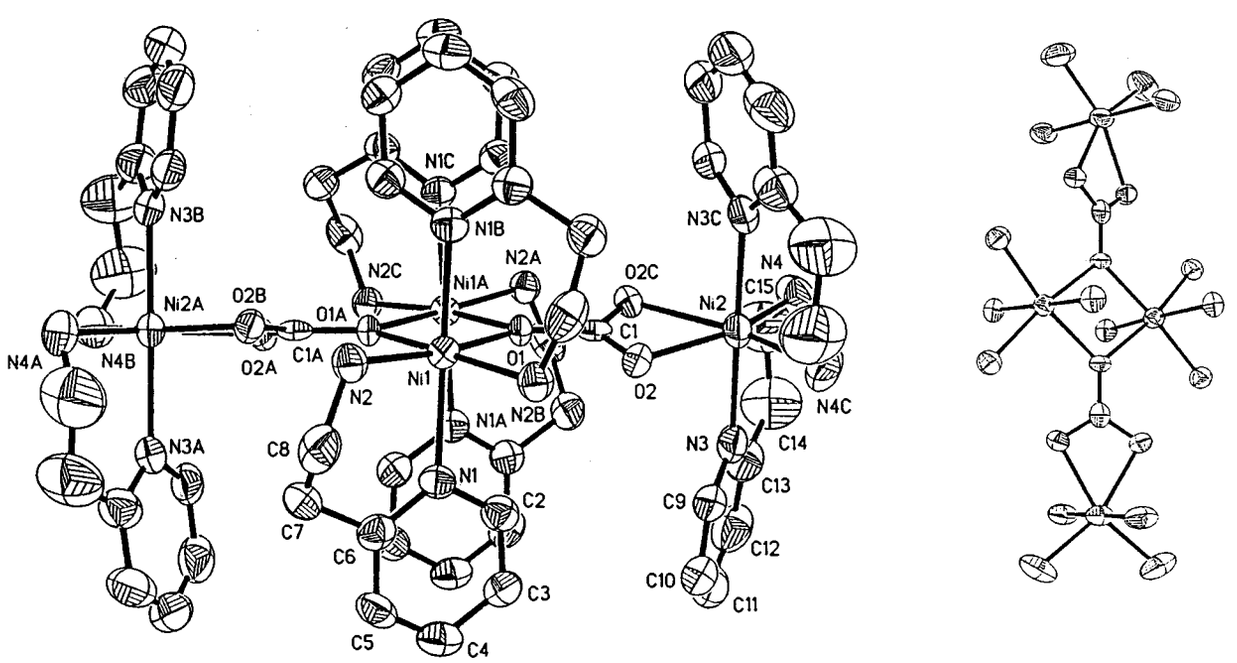

Fig. 1 An ORTEP[16] drawing of $[Ni_4(\mu\text{-}CO_3)_2(aetpy)_8][ClO_4]_4$ with atom labelling scheme. Thermal ellipsoids are drawn at 50% probability.

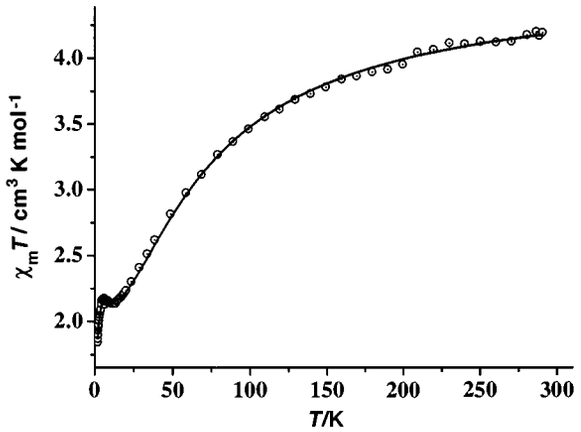

Fig. 2 Plot of $\chi_m T$ *vs.* T for $[Ni_4(\mu\text{-}CO_3)_2(aetpy)_8][ClO_4]_4$. The solid line shows the best fit obtained for the $J_{BB} = -31.8$, $J_{WB} = -7.0$, $J_{WW} = -0.36$ cm^{-1} coupling parameters. Fit obtained with eqn. (3) was indistinguishable in the 10–300 K range of temperatures.

O(1)–Ni(1A)–O(1A) ring [Ni(1)–Ni(1A) 3.468(1) Å], and the wings are formed by the Ni(2) environment, linked to the body by means of the O(2) and O(2C) atoms of the carbonate bridge [Ni(1) · · · Ni(2) 5.386(2) Å]. The Ni–CO_3–Ni_2–CO_3–Ni skeleton is not planar, because each carbonate plane is tilted with respect to the body of the complex; the dihedral angle between the two carbonate planes is 31.1(2)°.

Co-ordination of the (2-aminoethyl)pyridine ligands shows the usual bond parameters, but some features related with the carbonate bridges are relevant: the Ni(1)–O(1)–Ni(1A) bond angle is 105.3(2)°. The O(2)–Ni(2)–O(2C) bond angle of 61.9(2)° is similar to those found for bidentate co-ordination of the carbonate bridge.

Magnetic results

The plot of the $\chi_m T$ product *vs.* T is shown in Fig. 2. The $\chi_m T$ value at room temperature is 4.20 cm^3 K mol^{-1} which gradually decreases on cooling to reach a weakly pronounced minimum between 13 and 9 K (2.14 cm^3 K mol^{-1}); the 2.17 cm^3 K mol^{-1} value at 6.5 K abruptly decreases to 1.84 cm^3 K mol^{-1} at 1.9 K. This behaviour indicates a global antiferromagnetic interaction. Molar susceptibility increases with decreasing temperature over the whole range. Given the butterfly arrangement with D_{2h} symmetry of the four $S = 1$ local spins displayed in the studied compound, a preliminary analysis of the experimental susceptibility was performed by means of the Heisenberg-type Hamiltonian, eqn. (1), in which J_{WB}, J_{BB} and J_{WW} refer

$$H = -J_{WB}(S_1S_2 + S_1S_{2A} + S_{1A}S_2 + S_{1A}S_{2A}) - J_{BB}S_1S_{1A} - J_{WW}S_2S_{2A} \quad (1)$$

to the interactions wing–body, body–body and wing–wing respectively.

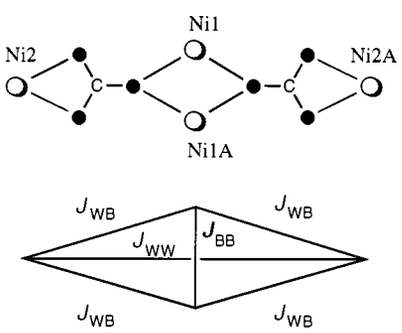

Assuming that the interaction between the terminal Ni2 and Ni2A is negligible and $J_{WW} = 0$, the eigenvalues of the spin Hamiltonian may be determined by using the Kambe vector coupling method[16] on the basis of the coupling shown in eqn. (2). The energies of the 19 spin states ranging from $S_T = 0$–4 may be obtained from eqn. (3).

$$S_A = S_1 + S_{1A};\ S_B = S_2 + S_{2A} \text{ and } S_T = S_A + S_B \quad (2)$$

$$E(S_TS_AS_B) = -J_{WB}/2[S_T(S_T + 1) - S_A(S_A + 1) - S_B(S_B + 1)] - J_{BB}/2S_A(S_A + 1) \quad (3)$$

The corresponding expression for the $\chi_m T$ product was derived from eqn. (3) using the Van Vleck equation, assuming an isotropic g value. Best fit parameters of the experimental data, in the 300–10 K range, were $J_{WB} = -7.9(1)$, $J_{BB} = -28.6(2)$ cm^{-1} and $g = 2.16$. From these data, the J_{WB}/J_{BB} ratio is 0.28.

These results are in good agreement with the expected values for the two superexchange pathways. The superexchange pathway between Ni(1) and Ni(1A) is a double monoatomic bridge with a Ni(1)–O(1)–Ni(1A) bond angle of 105.3°. The interaction between the magnetic orbitals of the nickel ions and the a_2 molecular orbital of the carbonate bridge is formally analogous to the superexchange pathway provided by one μ-hydroxo ligand. For this kind of bridge, the maximum antiferromagnetic coupling should be found for large Ni–O–Ni bond angles (close to 180°), and the interaction should decrease for lower angles. In good agreement with this prediction, previously reported carbonate bridges with Ni–O–Ni bond angles close to 180° show J values in the −78 to −94 cm^{-1} range,[4] and for a Ni–O–Ni bond angle of 141.4° $J = -57.7$ cm^{-1} was found.[4f] From the experimental value of 105.3° {Ni(1)–O(1)–Ni(1A) angle of $[Ni_4(\mu\text{-}CO_3)_2(aetpy)_8][ClO_4]_4$} a moderate antiferromagnetic interaction may be expected, in good agreement with $J_{BB} = -28.6$ cm^{-1}. Taking as reference other previously reported dinuclear systems showing the same kind of bidentate–monodentate co-ordination of the carbonate bridge between the two paramagnetic centres, weaker antiferromagnetic interaction is expected for the wing–body pathway, and excellent agreement with the $J = -7.8$ cm^{-1} value found for the dimeric unit $[(\mu\text{-}CO_3)\{Ni_2(dmpd)_4(H_2O)\}]^{2+}$ (dmpd = 2,2-dimethylpropane-1,3-diamine), should be pointed out.[3]

One of the most interesting features of the above susceptibility experiment is the $\chi_m T$ value of 2.2 cm^3 K mol^{-1} value at 4 K, which clearly indicates that in spite of the global antiferromagnetic interaction, $S_T = 0$, corresponding to $(S_TS_AS_B) = (0,0,0)$ is not undoubtedly the ground state. Several ground states or even spin frustration may be obtained for a butterfly arrangement of paramagnetic centres related by at least one antiferromagnetic interaction. The plot of the energy for the eigenstates obtained from eqn. (3) *vs.* the J_{WB}/J_{BB} ratio, assuming that J_{BB} is negative and the J_{WW} contribution is negligible, is shown in Fig. 3. All the $S_T = 0$, 1, 2, 3 or 4 ground states are possible from the adequate J_{WB} and J_{BB} values, and spin frustration may be found for the J_{WB}/J_{BB} ratios −2/3, −1/3, 1/2 and 1/1, which correspond to the crossing points between different multiplicity ground states. More interesting is the −1/3 to 1/2 range, for which three $S_T = 2$, 1 and 0 are formally degenerate. The best fit $J_{WB}/J_{BB} = 0.28$ value, lies in the region in which the $(S_TS_AS_B)$ states (2,0,2), (1,0,1) and (0,0,0) are degenerate; $S_A = 0$ for all of them implies antiparallel alignment of the spin vectors S_1 and S_{1A} according to the highest antiferromagnetic interaction and the different values for S_B indicate the competing interactions for S_2 and S_{2A}.

The real ground state may be modified by several factors such as zero field splitting or by the J_{WW} coupling constant. Calculations performed by means of the full-matrix diagonalisation CLUMAG program,[17] using the complete Hamiltonian indicated in eqn. (1) show that degeneracy among these three states may be broken by the sign of the J_{WW} interaction: (2,0,2) being the ground state for positive J_{WW} values, whereas (0,0,0) becomes the ground state for negative J_{WW} values, Fig. 4. A new

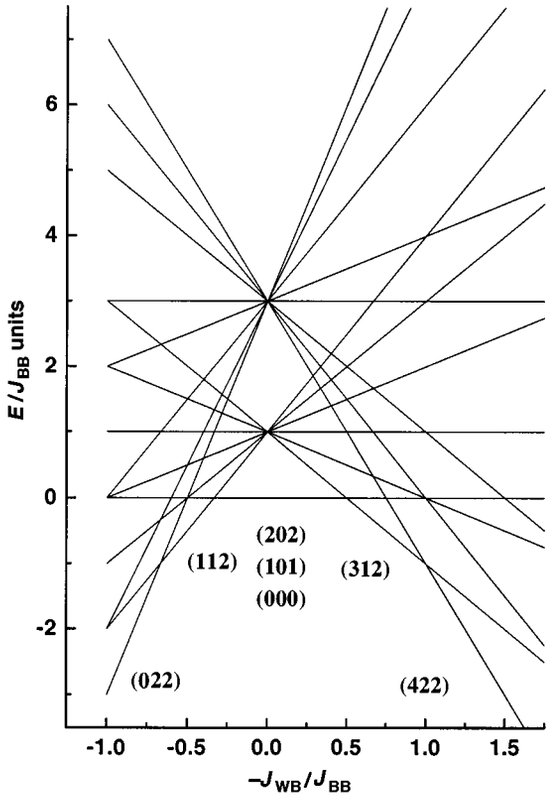

Fig. 3 Plot of the energy of the eigenstates ($S_TS_AS_B$) of a butterfly arrangement of four $S = 1$ local spins for different J_{WB}/J_{BB} values, for an antiferromagnetic J_{BB} interaction.

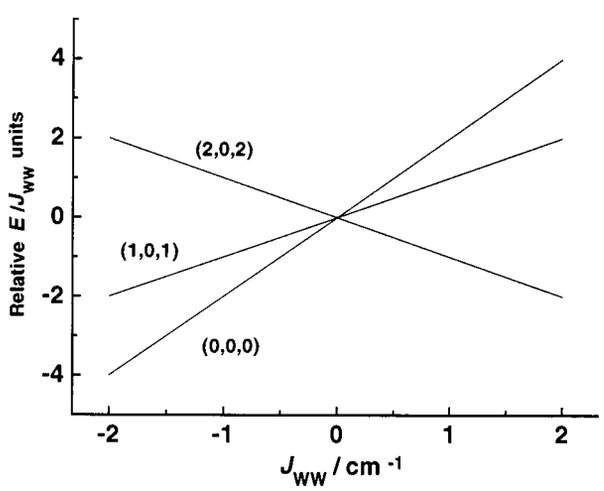

Fig. 4 Influence of J_{WW} on the degenerancy of the (0,0,0), (1,0,1) and (2,0,2) states, showing the stabilisation of (2,0,2) or (0,0,0) for positive or negative J_{WW} respectively.

fit taking into account the J_{WW} coupling constant with all experimental points, 300–1.9 K range of temperature, allows the best fit parameters of $J_{BB} = -31.8$, $J_{WB} = -7.0$, $J_{WW} = -0.36\ cm^{-1}$ and $g = 2.15$, $R = 4.9 \times 10^{-5}$, which corresponds to a J_{WB}/J_{BB} ratio of 0.22, Fig. 2.

Magnetisation experiments were performed at 6 and 1.9 K. The first measurement at 6 K shows an intermediate behaviour of $S = 1.57$, which corresponds to the mixing of the three possible ground states and eventually the closest excited state (1,1,2), Fig. 5. It is not possible from these measurements to assign the ground state unambiguously, but the found S_T value indicates without doubt the participation of the (2,0,2) state, taking into account that the next state with $S_T > 1$, (2,1,2), is placed at 20.7 cm^{-1} from the ground state. The measurement at 1.9 K is more informative: the weak increase for the magnetisation up to 5000 G indicates clearly that an $S = 0$ or almost an $M_S = 0$ is the ground spin level and the M/μ_B value of 2.2 found at 5 T shows that (2,0,2) also contributes to the global magnetisation even at 1.9 K. However, from this susceptibility or magnetisation experiment it is not possible to fully describe the energies involved in the ground state region. The above fits indicate that three spin levels are quasi-degenerate and that the inclusion of J_{WW} do not modify the situation. A very important factor has not been included: the zero field splitting of the $S = 1$ and $S = 2$ spin levels, which should be almost comparable to the gaps between $S = 0$, 1 or 2, mix the $M_S = 0$ from (0,0,0), $M_S = 0$ and $M_S = +/-1$ from (1,0,1) and $M_S = 0$, $+/-1$, $+/-2$ from (2,0,2). The sigmoidal shape of the magnetisation at 1.9 K is compatible with two possible ground states, (0,0,0) or (2,0,2) taking into account the zero field splitting. It is difficult to establish exactly the ground state, but on the other hand, this is the best proof for the quasi-ideal spin frustration behaviour for this compound.

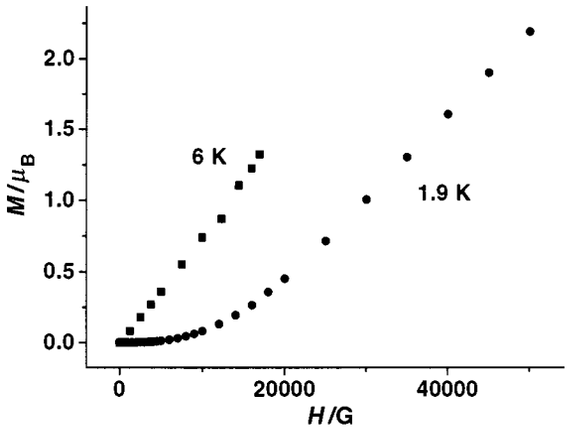

Fig. 5 Magnetisation measurement for $[Ni_4(\mu\text{-}CO_3)_2(aetpy)_8][ClO_4]_4$ showing the different response at 6 and 1.9 K.

Acknowledgements

A. E. and R. V. thank the CICYT (Grant PB096/0163) for support of this research. F. A. M. thanks Professor C. Kratky and Dr. F. Belaj (University of Graz) for use of experimental equipment. The authors are grateful to Professor F. Lloret (University of Valencia) for help in magnetic measurements.

References

1 J. Sletten, H. Hope, M. Julve, O. Kahn, M. Verdaguer and A. Dworkin, *Inorg. Chem.*, 1988, **27**, 542; N. Kitajima, T. Koda, S. Hashimoto, T. Kitagawa and Y. Moro-oka, *J. Am. Chem. Soc.*, 1991, **113**, 5664; R. Menif, J. Reibenspies and A. E. Martell, *Inorg. Chem.*, 1991, **30**, 3446; T. N. Sorrell, W. E. Allen and P. S. White, *Inorg. Chem.*, 1995, **34**, 952; P. E. Kruger, G. D. Fallon, B. Moubaraki, K. J. Berry and K. S. Murray, *Inorg. Chem.*, 1995, **34**, 4808; A. Escuer, R. Vicente, E. Peñalba, X. Solans and M. Font-Bardia, *Inorg. Chem.*, 1996, **35**, 3094; A. Escuer, E. Peñalba, R. Vicente, X. Solans and M. Font-Bardia, *J. Chem. Soc., Dalton Trans.*, 1997, 2315; A. Escuar, F. A. Mautner, E. Penalba and R. Vicente, *Inorg. Chem.*, 1998, **37**, 4190 and refs. therein.

2 T. Tanase, S. Nitta, S. Yoshikawa, K. Kobayashi, T. Sakurai and S. Yano, *Inorg. Chem.*, 1992, **31**, 1058.

3 A. Escuer, R. Vicente, S. B. Kumar, X. Solans and M. Font-Bardia, *J. Chem. Soc., Dalton Trans.*, 1997, 403.

4 (*a*) M. Mikuriya, I. Murase, E. Asato and S. Kida, *Chem. Lett.*, 1989, 497; (*b*) S. C. Rawle, C. J. Harding, P. Moore and N. W. Alcock, *J. Chem. Soc., Chem. Commun.*, 1992, 1701; (*c*) R. Kempe, J. Sieler, D. Walther, J. Reinhold and K. Rommel, *Z. Anorg. Allg. Chem.*, 1993, **619**, 1105; (*d*) K. Yamada, K. Hori and Y. Fukuda, *Acta Crystallogr., Sect. C*, 1993, **49**, 445; (*e*) N. Kitajima, S. Hikichi, M. Tanaka and Y. Moro-oka, *J. Am. Chem. Soc.*, 1993, **115**, 5496; (*f*) A. Escuer, R. Vicente, S. B. Kumar, X. Solans, M. Font-Bardia and A. Caneschi, *Inorg. Chem.*, 1996, **35**, 3094; F. Brezina,

Z. Smekal, Z. Sindelar and R. Pastorek, *Transition Met. Chem.*, 1997, **22**, 521.
5 G. Fachinetti and C. Floriani, *J. Am. Chem. Soc.*, 1979, **101**, 1767.
6 Some examples, H. Huang, F. Kai, Y. Asai, M. Hirohata and M. Nakamura, *Bull. Chem. Soc. Jpn.*, 1991, **64**, 2464; L. Ballester, E. Coronado, A. Gutierrez, A. Monge, M. F. Perpiñán, E. Pinilla and T. Rico, *Inorg. Chem.*, 1992, **31**, 2053; M. S. El Fallah, E. Rentschler, A. Caneschi and D. Gatteschi, *Inorg. Chim. Acta*, 1996, **247**, 231 and refs. therein.
7 H. J. Mai, H. C. Kang, S. Wocadlo, W. Massa and K. Dehnicke, *Z. Anorg. Allg. Chem.*, 1995, **621**, 1963; M. A. Halcrow, J. S. Sun, J. C. Huffman and G. Christou, *Inorg. Chem.*, 1995, **34**, 4167.
8 Some examples, A. J. Edwards, B. F. Hoskins, E. H. Kachab, A. Markiewicz, K. S. Murray and R. Robson, *Inorg. Chem.*, 1992, **31**, 3585; J. Ribas, M. Monfort, R. Costa and X. Solans, *Inorg. Chem.*, 1993, **32**, 695 and refs. therein.
9 C. J. Gomez-Garcia, J. J. Borrás-Almenar, E. Coronado and L. Ouahab, *Inorg. Chem.*, 1994, **33**, 4016.
10 M. Mikuriya, K. Nakadera and T. Kotera, *Bull. Chem. Soc. Jpn.*, 1996, **69**, 399.
11 N. Walker and D. Stuart, *Acta Crystallogr.*, *Sect. A*, 1983, **39**, 158.
12 G. M. Sheldrick, SHELXS 86, Program for the Solution of Crystal Structures, University of Göttingen, 1986.
13 G. M. Sheldrick, SHELXL 93, Program for the Refinement of Crystal Structures, University of Göttingen, 1993.
14 SHELXTL 5.03 (PC-Version), Program Library for the Solution and Molecular Graphics, Siemens Analytical Instruments Division, Madison, WI, 1995.
15 H. D. Flack, *Acta Crystallogr.*, *Sect. A*, 1983, **39**, 876.
16 C. K. Johnson, ORTEP, Report ORNL-5138, Oak Ridge National Laboratory, Oak Ridge, TN, 1976.
17 K. Kambe, *J. Phys. Soc. Jpn.*, 1950, **5**, 48.
18 D. Gatteschi and L. Pardi, *Gazz. Chim. Ital.*, 1993, **123**, 231.

Paper 8/03780I